ScienSage

Journal of Advanced Scientific Research

Available online through https://sciensage.info

ISSN: 0976-9595
Research Article
DOI: 10.55218/JASR.202213128

GRAPHENE OXIDE-MODIFIED V_2O_5 NANOPARTICLES: SYNTHESIS, CHARACTERIZATION AND MORPHOLOGICAL PROPERTIES

S.Kalaiarasi[1, 2], S. Shyamala[3], M. Kavitha[3], R. R. Muthuchudarkodi*[3]

[1]*Research scholar (Reg. No. 18222232032025), PG and Research Department of Chemistry V. O. Chidambaram College, Thoothukudi, Tamilnadu (Affiliated to Manonmaniam Sundaranar University, Tirunelveli, Tamilnadu), India*

[2]*PG and Research Department of Chemistry, A.P.C. Mahalaxmi College for Women, Thoothukudi, Tamilnadu, India*

[3]*PG and Research Department of Chemistry, V. O. Chidambaram College, Thoothukudi, Tamilnadu, India*

**Corresponding author: muthu.rajaram@gmail.com*

ABSTRACT

In the present investigation, reduced graphene oxide/Vanadium oxide (rGO/V_2O_5) nanocomposite was synthesized by the chemical synthesis method. Reduced Graphene oxide was synthesized by Hummer's method. rGO/V_2O_5 nanocomposite was also successfully synthesized using ammonium metavanadate as the source of vanadium. The crystalline structure, optical properties, and morphology of rGO/V_2O_5 nanocomposite were characterized by UV-VIS spectroscopy, IR spectroscopy, X-ray diffraction (XRD) studies, Photoluminescence (PL) spectroscopy and Field Emission Scanning Electron Microscope (FESEM) with EDAX spectroscopy. The optical property was analyzed using UV-Vis and Photoluminescence (PL) spectroscopy. The XRD spectrum showed diffraction peaks corresponding to the crystal planes of crystalline vanadium oxide. The XRD data confirms that V_2O_5 has an orthorhombic structure. The morphological studies of the nanocomposite revealed crystal-like morphology. The energy dispersive analysis confirmed the presence of Carbon, vanadium and oxygen in the doped rGO/V_2O_5 lattice. The PL results revealed the emission peak at 617nm and 397nm for V_2O_5 and rGO/V_2O_5 nanocomposite, respectively.

Keywords: rGO, V_2O_5, FESEM, XRD, Nanocomposite.

1. INTRODUCTION

Nanotechnology is the science of production, manipulation, and use of materials at the subatomic level to produce novel products and processes [1]. Recently, there has been great interest in fabricating and utilizing novel graphene oxide-metal oxide nanocomposites for environmental remediation by the degradation and elimination of toxic organic contaminants and heavy metals, and antibacterial applications. Compared to graphene oxide, graphene oxide-metal oxide nanocomposites show a unique structural morphology and photochemical properties which render them good candidates for water treatment projects [2]. Recently, many research groups are working on nanocomposite materials particularly graphene-based composite materials. Different types of graphene-based composite materials are being investigated and reported for various engineering applications [3].

The graphene obtained by reduction of graphene oxide still has many chemical and structural defects which are a problem for some applications but an advantage for some others [4]. In 1957, Hummers and Foeman developed a safer, quicker, and more efficient process called the hummers method, using a mixture of sulfuric acid H_2SO_4, sodium nitrate $NaNO_3$, and potassium permanganate $KMnO_4$, which is still widely used, often with some modifications [5-7]. Recently a mixture of H_2SO_4 and $KMnO_4$ has been used to cut open carbon nanotubes lengthwise, resulting in microscopic flat ribbons of graphene, a few atoms wide, with the edges "capped" by oxygen atoms (=O) or hydroxyl groups (-OH) [8]. Graphite (Graphene) oxide (GO) has also been prepared by using a "bottom-up" synthesis method (Tang-Lau method) in which the sole source is glucose, the process is safer, simpler, and more environmentally friendly compared to the traditionally "top-down" method, in which strong oxidizers are involved[9].

Among the various transition-metal oxides, V_2O_5 (VO) has widely been investigated as a high-potential candidate material because of the following merits: low cost, abundant resources, layered structure, high energy

density, and wide potential window arising from its multivalent oxidation states [10]. Although VO-based materials have achieved remarkable benchmark properties in various fields, such as in lithium-ion batteries, field-effect transistors, gas sensors, and supercapacitors, their poor electronic conductivity and bulk material properties prevent enhanced device performance [11,12]. Herein, we developed a simple one-step chemical synthesis process to prepare rGO/V_2O_5 nanocomposite. In this process, chemical reduction of graphene oxide into graphene and attachment of noble metal nanoparticles was achieved. These synthesized rGO/V_2O_5 nanocomposite employed were characterized by UV-VIS spectroscopy, IR spectroscopy, XRD,PL and Field Emission Scanning Electron Microscope (FESEM) with EDAX spectroscopy.

2. EXPERIMENTAL

2.1. Material

Graphite, Potassium permanganate, Phosphoric Acid, Hydrogen peroxide, ammonium metavanadate, Concentrated Hydrochloric Acid, potassium hydroxide, and deionized water were used to synthesize nanoparticles, Graphene oxide, and rGO/V_2O_5 nanocomposite.

2.2. Synthesis of V_2O_5 Nanoparticles

For synthesizing vanadium oxide nanoparticles, 0.1M solution of Ammonium metavanadate solution was prepared in-room atmosphere. After stirring this solution for 10 minutes, 0.1 M nitric acid (HNO_3) was added to the solution slowly. The solution color changed to deep red color. Under this condition, the solution was continuously stirred for 1 h. After that, the solution was kept at rest for 15 minutes to form the precipitate. The precipitate was collected by sucking unwanted residue solution and washed with DD water slowly to remove the residue. Afterward, it was dried on the hot plate for removing the excess water in the precipitate. After complete drying, the product was heated in a muffle furnace at 400°C for 4 h [13].

2.3. Synthesis of rGO/V_2O_5 Nanocomposite

Reduced Graphene oxide was synthesized by the modified Hummers method applying graphite powder. 0.2 g of rGO was dispersed in 100 mL water by ultrasonication up to 30 min to separate a single sheet of graphene oxide. To synthesize *in situ*, rGO/V_2O_5 nanocomposite, subsequently, 0.2M (100mL) of ammonium metavanadate was added and sonicated for another 30 min followed by dropwise addition of 1M potassium hydroxide solution under stirring for 1h. This mixture was stirred well and refluxed for 2 h, which resulted in the formation of black color rGO/V_2O_5 nanocomposite. The precipitate was separated from the reaction mixture, washed several times with deionized water, and followed by washing with ethanol to remove the impurities. Finally, the obtained product was dried at room temperature [14].

2.4. Characterization

The FT-IR spectra were recorded using a Shimadzu instrument. Computer-controlled JASCO V-530 was used to study UV-VIS spectral behavior. Photoluminescence (PL) spectra of the samples were recorded on a spectrofluorometer (JASCO, FP8300). The computer-controlled XRD system JEOL IDX 8030 was used to record the X-ray diffraction of samples. EDAX and FESEM measurements were carried by JEOL JSM-6700F field emission scanning electron microscope.

3. RESULTS AND DISCUSSION

3.1. UV- VIS Analysis

To study the optical property and bandgap energy the sample was characterized by UV-Vis absorbance spectra analysis. Fig.1 shows the UV-Vis absorbance spectra analysis of V_2O_5 nanoparticles and rGO/V_2O_5 nanocomposite. The spectra of the nanoparticles and nanocomposite (Fig.1) show the same absorption peak at 262 nm that can be attributed to the absorption of surface-attaching V_2O_5 nanoparticles. The blue shift of the peak was due to the close conjugation of the V_2O_5 nanoparticles and the graphene oxide sheets that resulted in rapid electron transfer and increased transition energy [15].

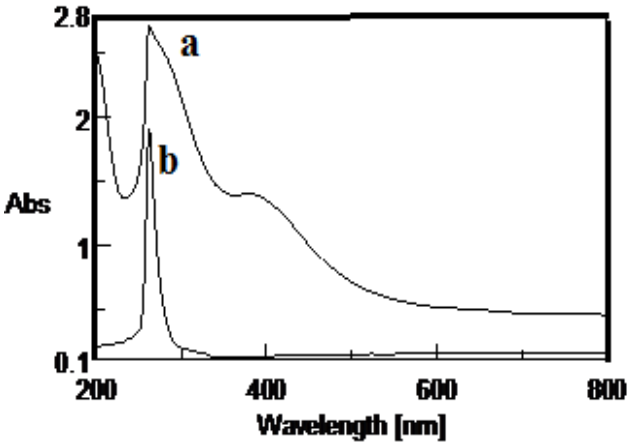

Fig. 1: UV-Visible absorbance spectra of a) V_2O_5 nanoparticles b) rGO/V_2O_5 Nanocomposite

The Tauc plot is used to calculate the optical band gap of V_2O_5 nanoparticles and rGO/V_2O_5 nanocomposite samples. An incident photon energy h is the relationship between the absorption coefficients. The following equation was used to calculate the optical band gap of a sample using Tauc's relation.

$$(\alpha h\upsilon)^2 = A(h\upsilon - Eg)$$

Where α denotes the absorption coefficient, *A* is constant, *Eg* is bandgap and exponent n depends on the type of transition. Fig.2 shows the optical band gap which was calculated using Tauc relation by plotting $(\alpha h\upsilon)^2$ against hυ, by extrapolating the straight-line portion of the curves to zero absorption coefficient value gives the energy band gap value. The bandgap energies calculated were 3.78 and 3.49eV for pure nano V_2O_5 and rGO/V_2O_5 nanocomposite respectively (Fig.2). Optical absorption study reveals the existence of several transitions at energies below the bandgap in V_2O_5 nanoparticles [14]. The observed decrease in bandgap energy can be attributed to the formation of the V_2O_5 between valance band to conduction band due to rGO doping [16].

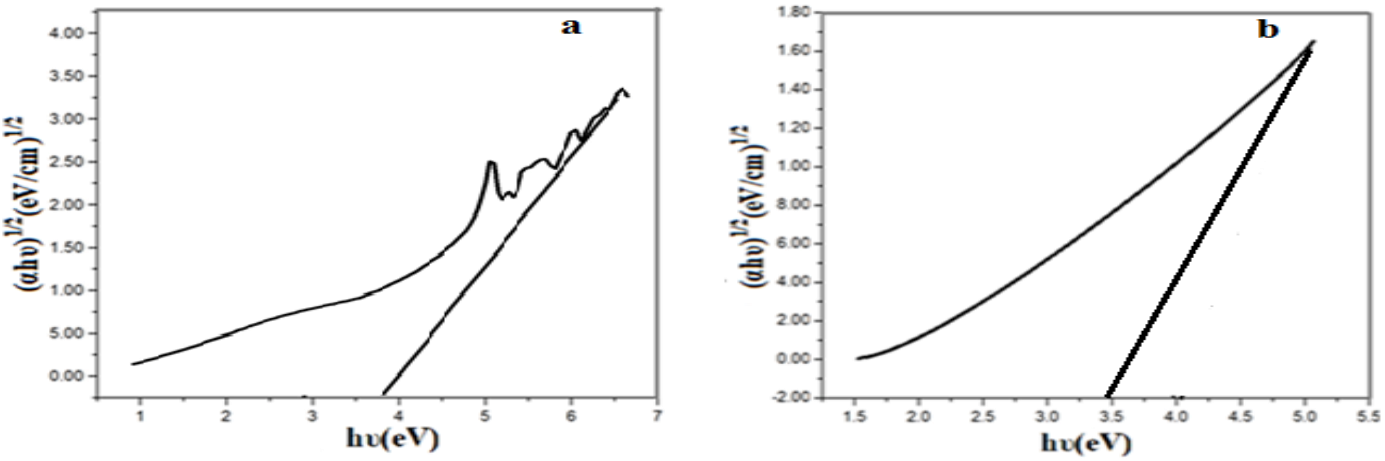

Fig. 2: Tauc plot of a) V_2O_5 nanoparticles b) rGO/V_2O_5 Nanocomposite

3.2. FTIR Analysis

FTIR spectra of the samples were analyzed which identifies the chemical bonds as well as functional groups in the compound. Fig. 3a shows FT-IR spectra of simple V_2O_5 nanoparticles. Fig.3a shows the large broadband at 3437cm^{-1} and 2923cm^{-1} which were ascribed to the O-H and C-H groups. The absorption peaks around 1400cm^{-1} is due to the bending vibration of C=C vibration. The bands between 532cm^{-1} and 769cm^{-1} correspond to metal-oxygen stretching which is endorsed to V-O-V symmetric stretch. The peak that appeared at 1004 cm^{-1} was assigned to vanadyl stretching modes (δ V-O). The peak at 1618 cm^{-1} was described as bending vibrations of water molecules [17-18].

FT-IR spectra of rGO/V_2O_5 nanocomposite are shown in Fig.3b.FT-IR spectra of rGO/V_2O_5 nanocomposite are exhibited broad absorption band at 3434 cm^{-1} is assigned to the O-H stretching vibration and indicating the presence of hydroxyl groups [19]. The FTIR spectrum for rGO/V_2O_5 nanocomposite is depicted in the figure which denotes the peaks corresponding to the wave numbers are 2369cm^{-1}, 1579cm^{-1}, 1118cm^{-1}, 669cm^{-1} denoting the presence of functional groups such as O=C=O, C=O, C-OH, O-V-O respectively. These functional groups indicate the presence of both V_2O_5 and rGO [20]. The IR spectrum of rGO/V_2O_5 nanocomposite has only one peak at 669 cm^{-1}, which is due to the stretching vibrations of V-O, confirming the formation of rGO/ V_2O_5 nanocomposite [21].

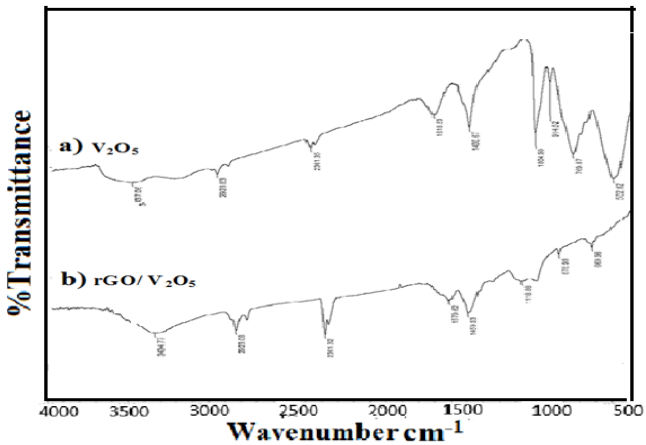

Fig. 3: FT-IR spectrum of a) V_2O_5 nanoparticles b) rGO/V_2O_5 nanocomposite

3.3. X-ray diffraction analysis

Structural properties of the prepared metal oxide nanoparticles and nanocomposite are studied by X-Ray Diffraction analysis. The crystallite size was calculated by using the Debye- Scherer formula

$$D=k\lambda/\beta\cos\theta$$

Where λ is the wavelength of radiation used (1.54060A° for Cu K radiation), k is the Scherrer constant equal to 0.94, β is the full width at half maximum (FWHM) intensity of the diffraction peak for which the particle size is to be calculated, θ is the diffraction angle of the concerned diffraction peak and D is the crystalline size in nanometers (nm).

The XRD pattern of the V_2O_5 nanoparticles and rGO/ V_2O_5 nanocomposite is shown in Fig.4. The XRD patterns showed (Fig: 4a) amorphous peaks with (011), (331), (002), and (322) diffraction planes, which are in agreement with the orthorhombic structure (JCPDS card no: 96-152-9745) of the V_2O_5 nanoparticles [22].

The XRD pattern of rGO/V_2O_5 nanocomposite is shown in Fig.4b. The sharp diffraction peaks suggested a well-crystalline nanomaterial. The XRD patterns showed crystalline peaks with (220) diffraction planes, which are in agreement with the orthorhombic structure (JCPDS card no: 96-432-7836) of the rGO/V_2O_5 nanocomposite [23]. Based on Scherrer's equation, the average crystalline size of the V_2O_5 and rGO/V_2O_5 nanocomposite is calculated and it was found to be 17.5nm and 39.4nm respectively.

3.4. FESEM and EDAX Analysis

Fig: 5 show the FESEM images and EDAX spectrum of V_2O_5 nanoparticles and rGO/V_2O_5 nanocomposite, respectively. The surface morphologies of synthesized V_2O_5 nanoparticles (Fig.5a) exhibit flowerlike in nature [3]. The EDAX spectrum, which exhibits the presence of two elements namely O and V.

Figure 5b shows that the V_2O_5 has uniformly merged onto the surface of the graphene oxide sheet. The EDAX pattern of rGO/V_2O_5 nanocomposite materials shown in the figure confirms that the synthesised materials show only C, O, and V elemental peaks. When compared to C and Elements, it is clear that a small amount of vanadium was obtained. The EDAX spectra confirm the presence of carbon as well as the rGO/V_2O_5nanocomposite [10].

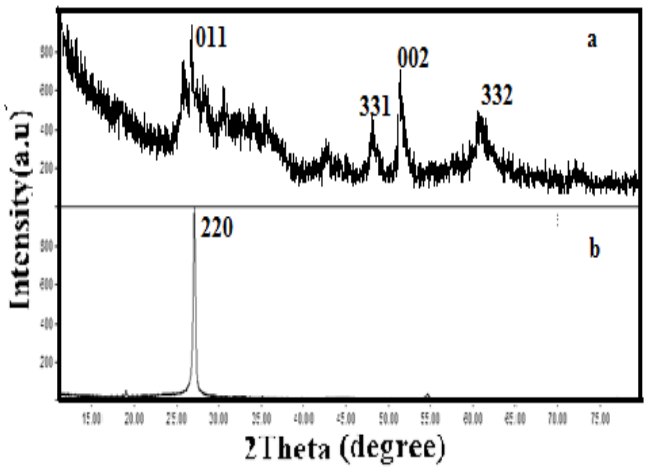

Fig. 4: XRD spectrum of a) V_2O_5 naoparticles b) rGO/V_2O_5 nanocomposite

3.5. Photoluminescence spectroscopy

The optical properties of V_2O_5 nanoparticles and rGO/V_2O_5 nanocomposite was analyzed (Fig.6) by using the photoluminescence (PL) spectral analysis. The excitation source employed here was the 262nm line of the Xe lamp.Fig.6 shows that pure V_2O_5 and rGO/ V_2O_5 nanocomposite has an emission peak at 617nm and 397nm. However, the emission peak of rGO/V_2O_5 nanocomposite is much lower than that of the pure V_2O_5, indicating that the addition of graphene will lead to the PL quenching.

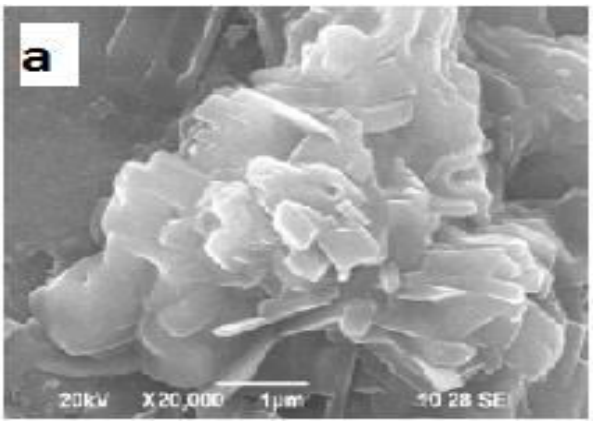

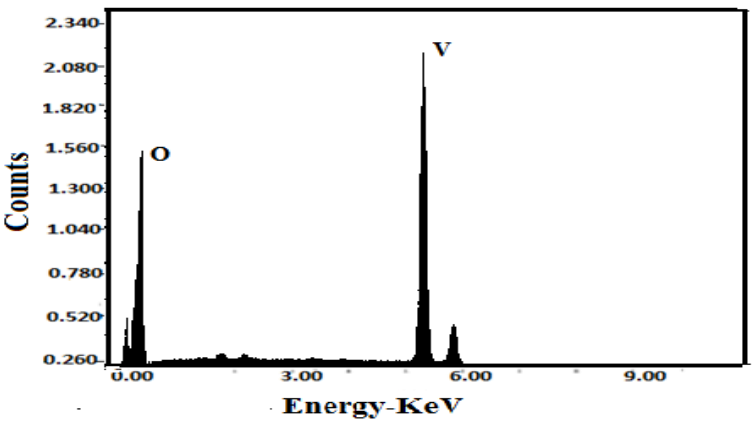

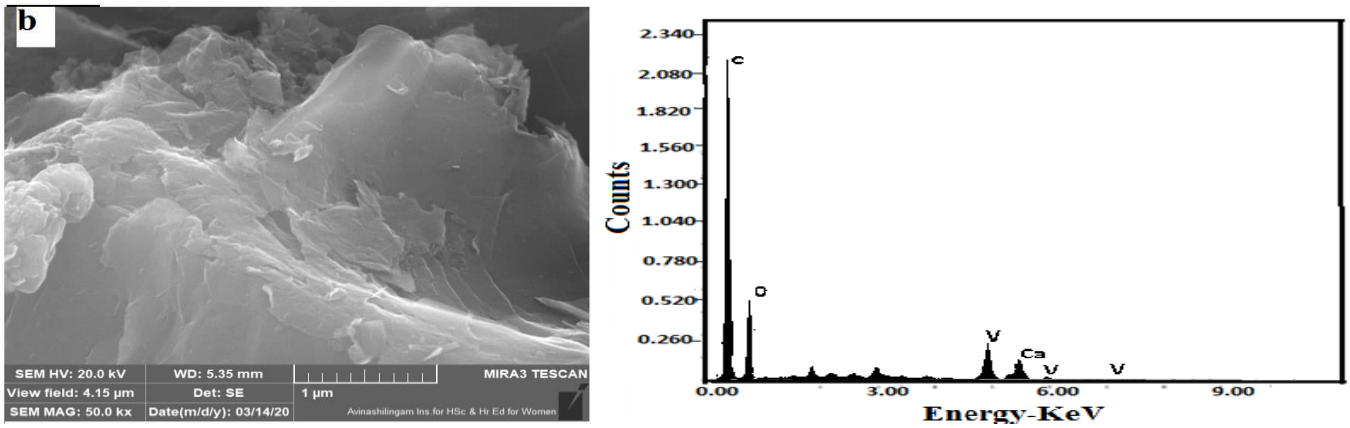

Fig. 5: FESEM images and EDAX spectrum of a) V_2O_5 nanoparticles b) rGO/V_2O_5 nanocomposite

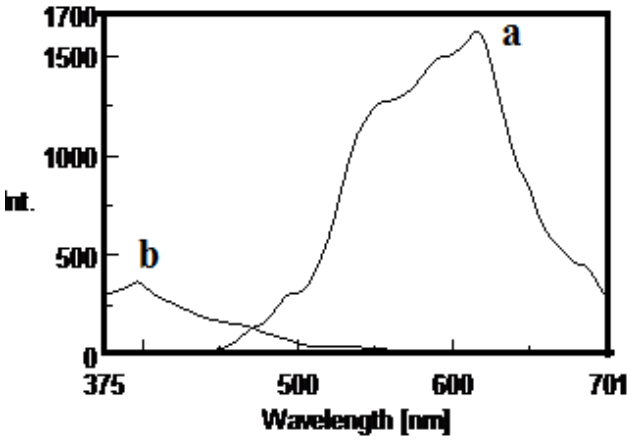

Fig. 6: Photo-luminescence (PL) spectra of a) V_2O_5 nanoparticles b) rGO/V_2O_5 nanocomposite

4. CONCLUSION

V_2O_5 nanoparticle and rGO/V_2O_5 nanocomposite have been successfully synthesized. The XRD spectra confirmed the formation of V_2O_5 and rGO/V_2O_5 samples. The X-Ray diffraction pattern confirms the phase purity of the synthesized nanocomposite. The effect of UV-Vis results showed that the bandgap energy decreased to about 3.78-3.49eV with the addition of doping concentrations in rGO. Surface functional groups present over V_2O_5 and rGO/V_2O_5 nano-composite were confirmed using FTIR. Surface morphological features with particle size, shape, and elemental analysis of nanocomposite are confirmed by FESEM and EDAX. PL spectra revealed the change of luminescence intensity in the rGO/V_2O_5 nanocomposite are compared to the V_2O_5 sample with almost a linear decrease in excitation intensity. The as-synthesized rGO/V_2O_5 nanocomposites resulted in improved structural and morphological characterization, as well as the investigation of a high performance Supercapacitor for future work.

5. ACKNOWLEDGEMENT

The authors are extremely grateful to PG and the Research Department of Chemistry, V.O.Chidambaram College, Thoothukudi for providing the Jasco V-530 UV-Visible Spectrophotometer, Spectrofluorometer, and FT-IR spectra. We are thankful to The Secretary of A.P.C Mahalaxmi College for women, Thoothukudi.

6. REFERENCES

1. Porter Alan L, Youtie Jan, Shapira Philip, Schoeneck David J. *J Nanopart Res,* 2008; **10**:715-728.
2. Li Q, Zhan Z, Jin S and Tan B. *Chem. Eng. J.,* 2017; **326:**109-116.
3. Chandra V, Park J, Chun Y, Lee WJ, Hang CI, Kim SK. *ACS Nano.,* 2010; **4**:3979.
4. Wei XD, Mao L, Soler-Crespo RA, Paci JT, Huang JX, Nguyen ST, Espinoza HD. *Nature Communications.*, 2015; **6**: 8029.
5. Hummers WS, Foeman RE. *Journal of the American Chemical Society*, 1958; **80(6)**:1339.
6. Kovtyukhova NI, Olivier PJ, Martin BJ, Mallouk TE, Chizhik SA,Buzaneva EV, et al. *Chemistry of Materials.*, 1999; **11 (3):** 771-778.
7. Marcano DC, Kosynkin DV, Berlin JM, Sinitskii A, Sun Z, Slesarev A, et al. *ACS Nano.*, 2010; **4(8)**:4806-4814.
8. Kosynkin DV, Higginbotham AL, Sinitskii A, Lomeda JR, Dimiev A, Price BK, Tour JM. *Nature,* 2009; **458(7240):**872-876.
9. Tang L, Li X, Ji R, Teng KS, Tai G, Ye J, Wei C, Lau SP. *Journal of Materials Chemistry.*, 2012; **22(12)**:5676.

10. Wee G, Soh HZ, Cheah YL, Mhaisalkar SG, Srinivasan M. *J. Mater. Chem.*, 2010; **20**:6720-6725.
11. Arico AS, Bruce P, Scrosati B, Tarascon JM, Van Schalkwijk W. *Nanostructured materials for advanced energy conversion and storage devices. Nat. Mater.*, 2005; **4**:366-377.
12. Perera SD et al., *Adv. Energy Mater*, 2011; **1**:936-945.
13. Nalini S, Selvakumar B, Periasamy P. *International Journal of Engineering and Manufacturing Science*, 2017; **7(2)**:411-417.
14. Nagi M et al., *RSC Adv.*, 2018; **8**:13323-13332
15. Yang Y, Liu TX. *Appli Surf Sci.*, 2011; **257(21)**:8950-8954.
16. Ganeshan S, Ramasundari P, Elangovan A, Arivazhagan G, Vijayalakshmi R. *International Journal of Scientific Research Physics and Applied Sciences*, 2017; **5(6)**:5-8.
17. Farahmandjou M, Abaeiyan N. *J. Nanomed Res.*, 2017; **5(1):** 00103.
18. Yang Y, Zhu QY, Jin AP, Chen W. *Solid State Ionics*, 2008; **179**:1250-1255.
19. Yugambica S, Clara Dhanemozhi A, Iswariya S. *International Research Journal of Engineering and Technology,* 2017; **04(02)**.
20. Saravanan T, Anandan P,Azhagurajan M, Arivanandhan M,Pazhanivel K, Hayakawa Y, Jayavel R. *Mater. Res. Express 3*, 2016; 075502,
21. Yuxin Tang, Xianhong Rui, Yanyan Zhang, Tuti Mariana Lim, Zhili Dong, Huey HoonHng, et al. *J. Mater. Chem.*, 2013; **A1:**82-88.
22. Cava RJ, Fleming RM, Santoro A, Murphy DW, Zahurak SM, Marsh P, Roth RS. *Journal of Solid State Chemistry,* 1986; **65**:63-71.
23. Yasuhito M, Kouji T, Takuya F, Hirofumi Y, Michio M, et al. *Inorganic Chemistry.,* 2012;**51**:456-462.